Event-Triggered Reliability Control for Fault Tolerant Tracking of Nonlinear Systems via Adaptive Dynamic Programming

Jian Liu, *Member, IEEE*, Jingjing Xia, Lijuan Zha, Jinliang Liu, *Senior Member, IEEE*, and Engang Tian, *Senior Member, IEEE*

***Abstract*—This study proposes a novel methodology driven by adaptive dynamic programming (ADP) to achieve optimal fault-tolerant tracking control (FTTC) in affine nonlinear systems subject to actuator failures. To begin with, a key innovation lies in constructing an extended system model that integrates tracking error dynamics and desired trajectory, establishing a basis for control synthesis. For this extended system, a critic neural network (NN) with adaptive weights is designed to approximate the discounted value function, enabling online optimization of control policies. In addition, to address practical network constraints, a bandwidth-efficient event-triggered scheme is introduced to optimize limited bandwidth resources in networked control setups. Meanwhile, an NN-based fault observer realizes real-time identification and dynamic compensation of actuator faults, mitigating their adverse effects on system performance. The resulting FTTC framework, which merges ADP-based optimal control with a fault compensator, ensures robust fault tolerance under both constant and time-varying fault scenarios. Through rigorous Lyapunov stability assessment, uniform ultimate boundedness is proven to be achieved for the closed-loop nonlinear system, guaranteeing stable tracking performance. The validity of this algorithm is verified through rigorous theoretical analysis and captivating numerical simulations.**

***Index Terms*—Adaptive dynamic programming (ADP), affine nonlinear systems (ANSs), event-triggered scheme, fault tolerant tracking control (FTTC), Hamilton–Jacobi–Bellman (HJB) equation.**

I. Introduction

RECENTLY, key components such as actuators and sensors are widely acknowledged to be prone to failures during operation, frequently leading to severe control failures or even system collapses [1], [2], [3]. Fault-tolerant control (FTC), as a core technology to enhance system reliability and safety, has thus attracted sustained attention in modern engineering systems, such as autonomous driving and industrial automation [4]. Existing FTC approaches can be categorized into active and passive types [5], [6]. To be specific, passive FTC relies on pre-designed robust controllers to handle known fault models as introduced in [7]: Mi et al.[7] designed a passive FTC for known fault models to compute ellipsoidal maximal tolerable fault sets, ensuring predefined feasible regions and ultimate bound requirements under additive fault models. However, system complexity may restrict its fault tolerant capability. Conversely, active FTC typically enables real-time fault diagnosis and control law switching, demonstrating better performance in detecting unknown faults compared to passive approaches. For example, Jiao et al. [8] used adaptive extended Kalman filter for error reduction and measurement noise weight adaptation over binary rejection for fault-tolerant navigation. As well as in a study by Bounemeur et al. [9], an adaptive active FTC approach via fuzzy logic and Nussbaum-type function is proposed to handle control problems with state-dependent actuator failures. Therefore, designing active FTC for such systems holds substantial theoretical and practical value for system reliability.

In traditional control scenarios, reinforcement learning (RL) has merged as an adaptive framework, boasting core of online strategy optimization and reduced reliance on exact models. It has thus found appliance in tasks, such as stochastic linear quadratic control [10], FTC [11], and trajectory tracking [12], [13], [14]. Aiming to satisfy dynamic and steady-state performance specifications while alleviating the peaking issue, Zhang et al. [12] focused on applying a closed-loop reference model guided by constrained RL for unknown continuous-time systems. Liu et al. [14] applied RL to optimal tracking of nonlinear networked control systems. However, general RL frameworks lack tight integration with optimal control theory, making them less targeted for nonlinear systems requiring equation. Meanwhile, standard RL frameworks still face dual challenges of dynamic uncertainties in solving Hamilton–Jacobi–Bellman (HJB) equation [15], [16], [17]. To address this gap, adaptive dynamic programming (ADP), a control-specific branch of RL, has been developed to directly target the HJB equation via

Received 16 September 2025; revised 9 December 2025; accepted 31 January 2026. Date of publication 3 February 2026; date of current version 20 February 2026. This work was supported in part by the National Natural Science Foundation of China under Grant 62001210, Grant 62373252, and Grant 62273174, and in part by the Young Elite Scientists Sponsorship Program by JSAST under Grant JSTJ-2025-452. Associate Editor: S. Yin.*(Corresponding author: Jinliang Liu.)*

Jian Liu and Jingjing Xia are with the School of Computer and Artificial Intelligence, Nanjing University of Finance and Economics, Nanjing 210023, China (e-mail: by.liujian@gmail.com; 1563928737@qq.com).

Lijuan Zha is with the School of Science, Nanjing Forestry University, Nanjing 210037, China (e-mail: zhalijuan@vip.163.com).

Jinliang Liu is with the School of Computer Science, Nanjing University of Information Science and Technology, Nanjing 210044, China (e-mail: liujinliang@vip.163.com).

Engang Tian is with the School of Optical-Electrical and Computer Engineering, University of Shanghai for Science and Technology, Shanghai 200093, China (e-mail: tianengang@163.com).

Digital Object Identifier 10.1109/TR.2026.3660832

value function approximation with core algorithms including policy iteration and value iteration. In light of this, applications of ADP have been investigated in optimal control tasks such as adaptive optimal tracking control [18], [19], FTC [20] and battery management [21], [22]. For instance, the efficiency of ADP with parallel control to handle uncertainties is verified in [19]. To manage asymmetric inputs and guarantee safety-optimal performance, Zhang et al. [20] adopted ADP for FTC in unknown nonlinear systems. Building on this, we propose a gradient descent (GD)-driven ADP framework, integrating a critic-only neural network (NN) generalization and GD-based online optimization to dynamically update critic network parameters and enhance solution efficiency.

In addition, with the advancement of intelligent systems, tracking control gains prominence in robotic motion planning, unmanned aerial vehicle formation, and autonomous driving [23], [24]. In recent years, to tackle multisource disturbances and communication delays, scholars have proposed tracking methods integrating model predictive control and adaptive strategies under different control frameworks [25], [26], [27]. To achieve high-precision nonlinear tracking of autonomous vehicles, Meng et al. [25] optimized model predictive control in trajectory tracking systems with convergence criteria. In a study by Peng et al. [26], a controller tolerating a large delay upper bound and suppresses exogenous disturbances was designed via optimizing the robust performance index. Besides, Zeng et al. [27] achieved robust tracking control through integrating model prediction and adaptive strategies in nonlinear networked systems. However, existing studies rarely consider trajectory tracking and FTC simultaneously, though both are critical for practical systems. Our focus is on developing a high-performance tracking control in ADP to ensure reliable tracking under minimal cost and maximum disturbances. Existing single-performance research focuses on optimization, while fault tolerant tracking control (FTTC) coordination is underexplored, failing practical needs, such as industrial robotics. Thus, coordinating them to enhance robustness under resources is a key direction requiring urgent breakthroughs.

Against the backdrop of limited bandwidth in networked control systems, traditional time-triggered periodic sampling generates steady-state computations, exacerbating bandwidth consumption and impeding dynamic responses. Event-triggered control (ETC) emerges as a promising solution [28], [29], transmitting signals only when predefined triggering conditions are met [30], [31], [32]. However, most existing ETC designs prioritize stability over bandwidth optimization, leaving resource allocation suboptimal. Recent work such as Liu et al.'s [33] work has integrated ADP with event-triggered frameworks to reduce communication burden. Specifically, some of these works adopt a relative threshold mechanism that triggers control updates only when transmission errors exceed a dynamically adjusted threshold, combined with a multigradient recursive ADP algorithm. Nevertheless, these approaches often rely on conservative stability margins for threshold updates, failing to fully exploit the bandwidth-performance tradeoff. To bridge this gap, this article designs an adaptive triggering strategy that incorporates tracking errors into decision-making, reducing communication frequency while enhancing system performance to overcome the traditional safety-resource efficiency dilemma of ETC.

Building on the prior analysis, the research introduces an event-triggered FTTC framework integrating ADP to tackle the optimization challenge of nonlinear affine systems experiencing actuator faults under bandwidth-constrained environments. In contrast to preceding studies, the primary contributions of the present work are outlined in the following.

1) A novel bandwidth-efficient event-triggered scheme (BEETS) with adaptive conditions is proposed, where an ADP algorithm optimizes tracking control to balance optimality and bandwidth efficiency. Unlike [18] and [19] focusing only on stability, it eliminates redundant data transmission via threshold adjustment, ensuring tracking errors achieve uniform ultimate boundedness (UUB) while fitting real-world networked systems with limited resources.
2) An extended system model integrating tracking errors and desired trajectories into a unified state is constructed to handle actuator faults, different from typical tracking controls neglecting faults [12], [26], [27]. By unifying them as state vectors, it systematically enables fault-tolerant law design, enhancing robustness against time-varying actuator faults and ensuring reliable tracking under faulty conditions.
3) A data-driven ADP-based NN fault observer realizes real-time compensation for unknown actuator faults, overcoming the limitation of existing passive FTC methods in [7] that rely on known fault models. Moreover, it dynamically adjusts weights via Lyapunov-stable online tuning, addressing unknown faults, such as partial or total effectiveness loss.

The rest of this article is organized as follows. Section II models for actuator-faulty nonlinear systems and designs the HJB equation under event-triggered mechanisms. Section III develops a fault-tolerant tracking controller for fault estimation and compensation, while introducing a GD-driven ADP iterative algorithm to achieve optimal control. Section IV validates the proposed method through extensive simulations. Finally, Section V concludes this article.

II. Preliminaries and Problem Identification

Within this section, we first describe the system subject to actuator failures and the reference model. Subsequently, the event-triggered fault-resilient tracking control problem will be investigated grounded in optimal control theory via Bellman's approach.

A. System Statement

We model the continuous-time affine nonlinear systems (ANSs) subject to actuator faults as follows:

$$\dot{x}(t) = f(x(t)) + g(x(t))(u(t) - u_f(t)) \tag{1}$$

in which $x(t) \in \Re^n$ and $u(t) \in \Re^m$ are in correspondence with the system state vector and control input vector, respectively;

$f(\cdot)$ stands for the known nonlinear internal function, and $g(\cdot)$ is the input gain function.

Assumption 1: Both the known terms $f(\cdot)$ and $g(\cdot)$ comply with globally Lipschitz continuity and differentiability in their domains. In addition, it is assumed that $f(0) = 0$ as a standard initial condition.

Assumption 2 (See [34]): The actuator failure u_f is subject to norm bounds, in which its magnitude and time derivative are constrained as $\|u_f(t)\| \leqslant \rho_1$ and $\|\dot{u}_f(t)\| \leqslant \rho_2$, respectively. Here, ρ_1 and ρ_2 are two predefined positive constants denoting the upper bounds for the failure and its rate of change.

Remark 1: System control ability is a foundational assumption within the control field. Moreover, referring to [35], it is noteworthy that Assumption 1 is reasonable on the condition that applied input can transfer the system from any initial state $x(t_0)$ to any state $x(t_1)$ for $t_1 > t_0$. This is rooted in the controllability principle, which guarantees reachability from any starting point.

Considering $d(t) \in \Re^n$ is the target trajectory, which is predefined as a smooth nonlinear function at least continuously differentiable of order 1, one can construct a continuous nonlinear function $\phi(d(t))$ that meets

$$\dot{d}(t) = \phi(d(t)).$$

Let $u_d \in \Re^m$ be the desired control input, where the system dynamic is given by

$$\dot{d}(t) = f(d(t)) + g(d(t))u_d(t).$$

Therefore, we can get

$$u_d(t) = g^{\circ}(d(t))(d(t) - f(d(t)))$$

where $g^{\circ}(\cdot)$ stands for the Moore–Penrose pseudoinverse of $g(\cdot)$. Then, we introduce the tracking error term as $\epsilon(t) = x(t) - d(t)$, with its temporal derivative derived as

$$\dot{\epsilon}(t) = \dot{x}(t) - \dot{d}(t). \tag{2}$$

The central purpose of this article is to develop an FTTC strategy grounded in ADP, aiming to maintain the trajectory-tracking efficacy of nonlinear systems even when actuator faults occur. In other words, the proposed ADP-driven FTTC approach can ensure that closed-loop nonlinear systems with actuator imperfections are stable in terms of UUB, thereby upholding system performance integrity under actuator fault scenarios.

B. Problem Description

Regarding the system in fault-free scenario, we construct the control error input $u_\epsilon(t)$ to minimize the performance index criterion

$$\jmath(\epsilon(t)) = \int_0^{\infty} (\epsilon^T(\tau)Q\epsilon(\tau) + u_\epsilon^T(\tau)Ru_\epsilon(\tau)d\tau$$

where $u_\epsilon(t) = u(t) - u_d(t)$; state weighting matrix $Q \in \Re^{n\times n}$ and control input weighting matrix $R \in \Re^{m\times m}$ are both symmetric positive-definite matrices. In order to effectively address FTTC problem, an NN-based fault estimator is developed to identify actuator fault. Moreover, the control law requires adaptive compensation to account for these failures, ensuring robust performance under actuator degradations.

Then, we define $\epsilon(t) = x(t) - d(t)$ and denote $\chi(t) = [\epsilon(t)^T, d(t)^T]^T \in \Re^{2n}$. Thus, with respect to the faultless system, the extended system state is constructed as

$$\dot{\chi}(t) = \boldsymbol{F}(\chi(t)) + \boldsymbol{G}(\chi(t))\mu(t) \tag{3}$$

in which $\mu(t) \in \Re^m$ represents the control input for the nonfaulty extended system [36]. The matrices $\boldsymbol{F}(\chi(t))$ and $\boldsymbol{G}(\chi(t))$ are structured as $\boldsymbol{F}(\chi(t)) = \begin{bmatrix} f(\epsilon + d) - \phi(d) \\ \phi(d) \end{bmatrix}$, $\boldsymbol{G}(\chi(t)) = \begin{bmatrix} g(\epsilon + d) \\ 0 \end{bmatrix}$.

On the basis of the extended system (3), a performance index function is first formulated as

$$\jmath(\chi(t)) = \int_t^{\infty} e^{-\Upsilon(\tau - t)} \left(\chi^T(\tau)\bar{Q}\chi(\tau) + \mu(\tau)^T R\mu(\tau)\right) d\tau \tag{4}$$

in which $0 < \Upsilon \leq 1$ denotes the discount factor, $\bar{Q} = \begin{bmatrix} Q & 0 \\ 0 & 0 \end{bmatrix} \in \Re^{2n\times 2n}$ and the exponential term $e^{-\Upsilon(\tau-t)}$ [37] is incorporated to guarantee the convergence of $\chi(t)$.

Remark 2: Focusing on the constructed extended system (3), the goal of the nonfaulty system tracking control is transformed into finding control law μ to reduce the performance index function (4) to its minimum. Notably, $\mu(t)$ consists of specific components including the target control input $u_d(t)$ and the control error term $u_\epsilon(t)$. Meanwhile, $\mu(t)$ needs to adhere to the admissibility criteria.

Definition 1: Using the tracking error dynamics described in (2), let $\Omega \in \Re^n$ represent a continuous admissible set for $\mu(t)$, with $\mu(0)$ starting from zero as the initial value. This set ensures both the stability of system (2) and the finiteness of performance index (4) for every $\chi(t)$ within Ω.

For any control law $\mu(t) \in ß(\Omega)$, in which $ß(\Omega)$ is the set of all admissible control actions that satisfy the operational constraints of the system, a continuously differentiable value function is derived from [37] as

$$\mathcal{V}(\chi(t)) = \int_t^{\infty} e^{-\Upsilon(\tau-t)}(\chi^T(\tau)\bar{Q}\chi(\tau) + \mu^T(\tau)R\mu(\tau))d\tau. \tag{5}$$

Next, we desire to utilize a Hamiltonian function for addressing the tracking control problem in depth, with the optimal value function systematically expressed as

$$\begin{aligned} &H(\chi(t), \mu(\chi), \nabla\mathcal{V}(\chi(t))) \\ &= \chi^T(t)\bar{Q}\chi(t) + \mu^T(\chi)R\mu(\chi) - \Upsilon\mathcal{V}(\chi(t))) \\ &\quad + (\nabla\mathcal{V}(\chi(t)))^T\dot{\chi}(t) \end{aligned}$$

and

$$\mathcal{V}^*(\chi) = \min_{\mu\in ß(\Omega)} \int_t^{\infty} e^{-\Upsilon(\tau-t)}(\chi^T\bar{Q}\chi + \mu^T R\mu)d\tau$$

in which $\nabla\mathcal{V}(\chi)$ stands for the partial derivative vector of $\mathcal{V}(\chi)$, i.e., $\nabla\mathcal{V}(\chi) = \partial\mathcal{V}/\partial\chi$ and the HJB equation, fundamental

to optimal control design, satisfies $\min_{\mu\in\mathfrak{B}(\Omega)} H(\chi(t),\mu(\chi), \nabla\mathcal{V}^*(\chi(t))) = 0$.

Referring to Pontryagin's minimum principle, we obtain

$$\frac{\partial H}{\partial \mu} = 2R\mu(t) + \boldsymbol{G}^T(\chi(t))\nabla\mathcal{V}^*(\chi(t)). \tag{6}$$

Subsequently, describe the optimal control input strategy as follows:

$$\begin{aligned}\mu^*(\chi(t)) &= \arg\min_{\mu\in\mathfrak{B}(\Omega)} H(\chi(t),\mu(\chi(t)),\nabla\mathcal{V}^*(\chi(t)))\\ &= -\frac{1}{2}R^{-1}\boldsymbol{G}^T(\chi(t))\nabla\mathcal{V}^*(\chi(t)).\end{aligned} \tag{7}$$

Based on $\mu^*(\chi)$, the HJB equation is revised to incorporate this input, yielding

$$\begin{aligned}&\min_{\mu\in\mathfrak{B}(\Omega)} H(\chi(t),\mu(\chi(t)),\nabla\mathcal{V}^*(\chi(t)))\\ &= \chi^T(t)\bar{Q}\chi(t) + (\mu^*(\chi(t)))^T R\mu^*(\chi(t)) - \Upsilon\mathcal{V}(\chi(t)))\\ &\quad + (\nabla\mathcal{V}^*(\chi(t)))^T(\boldsymbol{F}(\chi(t)) + \boldsymbol{G}(\chi(t))\mu^*(t))\\ &= 0.\end{aligned} \tag{8}$$

In response to the critical challenge of limited network bandwidth, this article devises a BEETS to strike a balance between communication efficiency and control precision. More specifically, data transmission attains peak efficiency precisely when the subsequent event-triggered condition is rigorously validated

$$l_s^T(t)\Omega l_s(t) > \chi^T(t_s+nT)\Omega\chi(t_s+nT) \tag{9}$$

in which $l_s(t) = \chi(t_s+nT) - \chi(t_s)$ with $n\in\{1,2,3,\ldots\}$. The event-triggered instants t_s with $t_0 = 0$ is a multiple of sampling period T; Ω denotes a symmetric positive weight matrix; $\chi(t_s)$ and $\chi(t_s+nT)$ represent data transmitted at t_s and the latest sampled data respectively. Hence, the subsequent triggering instant t_{s+1} can be formulated as

$$t_{s+1} = t_s + \min_{n\geq 1}\{nT | nT \text{ satisfying Eq. (9)}\}. \tag{10}$$

Remark 3: The Zeno behavior is inherently excluded by the design of a strictly positive minimum event-triggered interval. Given the periodic sampling of the system state, the minimum interval between any two consecutive triggering instants is on less than one sampling period T. This ensures triggering intervals cannot approach zero, thereby avoiding the Zeno phenomenon.

Under the BEETS, the value of the control input $\mu(\chi(t))$ remains constant at two adjacent event-triggering instants t_s and t_{s+1}, i.e., $\mu(\chi(t)) = \mu(\chi(t_s))$. Based on the characteristic, the optimal control input strategy in (7) can be further rewritten as

$$\begin{aligned}\mu^*(\chi(t)) &= \mu^*(\chi(t_s))\\ &= -\frac{1}{2}R^{-1}\boldsymbol{G}^T(\chi(t_s))\nabla\mathcal{V}^*(\chi(t_s))\end{aligned} \tag{11}$$

where $t\in[t_s,t_{s+1})$. Based on BEETS, the HJB equation is modified as

$$\begin{aligned}&H(\chi(t),\mu^*(\chi(t_s)),\nabla\mathcal{V}^*(\chi(t)))\\ &= \chi^T(t)\bar{Q}\chi(t) + (\mu^*(\chi(t_s)))^T R\mu^*(\chi(t_s)) - \Upsilon\mathcal{V}(\chi(t)))\\ &\quad + (\nabla\mathcal{V}^*(\chi(t)))^T(\boldsymbol{F}(\chi(t)) + \boldsymbol{G}(\chi(t))\mu^*(t_s))\\ &= 0, \qquad t\in[t_s,t_{s+1}).\end{aligned} \tag{12}$$

Remark 4: The event-triggered scheme (9) designed in the article is intended to optimize bandwidth resources. Namely, the control policy $\mu(t)$ updates itself to transmit sampled data when the event-triggering condition (9) is satisfied. Under such a mechanism, this article endeavors to prove that the constructed extended system is UUB.

III. Solution to Optimal FTTC Through ADP

Owing to the challenge of deriving an analytical solution for the event-triggered HJB equation in (12), an ADP-driven effective algorithm is developed to estimate the solution. In accordance with the event-triggered protocol defined in (9), the control policy remains constant between consecutive event-triggering instants. Thus, in the remainder of this article, we adopt $u^*(\chi_s)$ without explicit mention of $t\in[t_s,t_{s+1})$ unless otherwise specified.

A. ADP-Based Critic NN Implementation

Before presenting the iterative algorithm, for the sake of conciseness in the subsequent description, we denote $\chi(t)$, $\chi(t_s)$, $l_s(t)$, $d(t)$ as χ, χ_s, l_s, d, respectively.

The value function $\mathcal{V}(\chi)$ is estimated by using the following single-layer NN:

$$\mathcal{V}^*(\chi) = W_c^T\varphi(\chi) + \varepsilon_c(\chi) \tag{13}$$

with $W_c\in\Re^{l_c}$ representing the ideal weight vector, $\varphi(\chi)$ denoting the activation function and $\varepsilon_c(\chi)\in\Re$ standing for the approximation error, where l_c is the number of hidden layer neurons.

Correspondingly, the partial gradient of $\mathcal{V}(\chi)$ with respect to the extended system χ is

$$\nabla\mathcal{V}^*(\chi) = \nabla\varphi^T(\chi)W_c + \nabla\varepsilon_c(\chi). \tag{14}$$

Then, the optimal tracking control policy in (7) and the Hamiltonian can be obtained as

$$\begin{aligned}\mu^*(\chi) &= \mu^*(\chi_s)\\ &= -\frac{1}{2}R^{-1}\boldsymbol{G}^T(\chi_s)\nabla\mathcal{V}^*(\chi_s)\\ &= -\frac{1}{2}R^{-1}\boldsymbol{G}^T(\chi_s)(\nabla\varphi^T(\chi_s))W_c + \nabla\varepsilon_c(\chi_s))\end{aligned} \tag{15}$$

and

$$\begin{aligned}&H(\chi,\mu^*(\chi_s),W_c)\\ &= \chi^T\bar{Q}\chi + (\mu^*(\chi_s))^T R\mu^*(\chi_s) - \Upsilon W_c^T\varphi(\chi)\\ &\quad + W_c^T\nabla\varphi(\chi(t))\dot{\chi} + Z_H\\ &= 0\end{aligned} \tag{16}$$

where $Z_H = -\Upsilon\varepsilon_c(\chi) + \nabla\varepsilon_c^T(\chi)\dot{\chi}(t)$ stands for the residual error.

In fact, the exact value of W_c is hard to approximate. Given to the unknown, we adopt the following equation to obtain its

actual weight:

$$\hat{\mathcal{V}}(\chi) = \hat{W_c}^T \varphi(\chi). \tag{17}$$

Next, the partial gradient of $\hat{\mathcal{V}}(\chi)$ is estimated as

$$\nabla\hat{\mathcal{V}}(\chi) = \nabla\varphi^T(\chi)\hat{W}_c. \tag{18}$$

Therefore, the approximate value of the optimal tracking control input denoted by $\hat{\mu}(\chi)$ can be given as

$$\begin{aligned}\hat{\mu}(\chi(t)) &= \hat{\mu}(\chi_s)\\ &= -\frac{1}{2}R^{-1}\boldsymbol{G}^T(\chi_s)\nabla\varphi^T(\chi_s)\hat{W}_c.\end{aligned} \tag{19}$$

The above-mentioned strategy can obtain an approximate Hamiltonian, that is

$$\begin{aligned}&\hat{H}(\chi, \hat{\mu}(\chi_s), \hat{W}_c)\\ &= \chi^T\bar{Q}\chi + \hat{\mu}^T(\chi_s)R\hat{\mu}(\chi_s) - \Upsilon\hat{W_c}^T\varphi(\chi)\\ &\quad + \hat{W_c}^T\nabla\varphi(\chi)\dot{\chi}.\end{aligned} \tag{20}$$

We then denote the approximation error between $\hat{H}(\cdot)$ and $H(\cdot)$ as g_h, and thus it is derived that

$$\begin{aligned}g_h &= \hat{H}(\chi, \hat{\mu}(\chi_s), \hat{W}_c) - H(\chi, \mu^*(\chi_s), W_c)\\ &= \hat{W_c}^T\delta + \chi^T\bar{Q}\chi + \hat{\mu}^T(\chi_s)R\hat{\mu}(\chi_s)\end{aligned} \tag{21}$$

where $\delta = \nabla\varphi(\chi)\dot{\chi} - \Upsilon\varphi(\chi)$.

In order to estimate W_c effectively by $\hat{W}_c$, we need to achieve the value of $\mu^*(\chi)$ as g_h approaches zero. For the purpose, we define an objective function

$$E = \frac{1}{2(1+\delta^T\delta)^2}g_h^T g_h. \tag{22}$$

Inspired by gradient decent algorithm, we obtain

$$\begin{aligned}\dot{\hat{W}}_c &= -l_h\frac{\partial E}{\partial\hat{W}_c} = -l_h\frac{\partial E}{\partial g_h}\frac{\partial g_h}{\partial\hat{W}_c}\\ &= -l_h\frac{1}{(1+\delta^T\delta)^2}\frac{\partial g_h}{\partial\hat{W}_c}.\end{aligned}$$

Since $\frac{\partial g_h}{\partial\hat{W}_c} = \delta - \hat{\mu}^T\boldsymbol{G}^T(\chi_s)\nabla\varphi^T(\chi_s)$ and $\hat{\mu}$ satisfies the approximate optimality condition that the gradient of the Hamiltonian with respect to μ is zero, we have $\frac{\partial g_h}{\partial\hat{W}_c} = \delta$. Consequently, $\hat{W}_c$ is updated by

$$\dot{\hat{W}}_c = -l_h\frac{\delta}{(1+\delta^T\delta)^2}g_h \tag{23}$$

in which the learning rate l_h can influence the convergence behavior of the algorithm. Then, we define $\tilde{W}_c = W_c - \hat{W}_c$ as the weight approximated error and thereby we derive that

$$\dot{\tilde{W}}_c = -l_h\frac{\delta\delta^T}{(1+\delta^T\delta)^2}\tilde{W}_c + l_h\frac{\delta}{(1+\delta^T\delta)^2}\varsigma_c \tag{24}$$

in which $\varsigma_c = -(\nabla\varepsilon(\chi(t)))^T\dot{\chi}(t) + \Upsilon\varepsilon(\chi(t))$ represents the residual error.

Based on the updating law (23), $\hat{W}_c$ can be calculated at time t

$$\begin{aligned}\hat{W}_c(t) &= \hat{W}_c(t-T)\\ &\quad - l_hT\frac{\delta(t-T)}{(1+\delta^T(t-T)\delta(t-T))^2}g_h(t-T).\end{aligned} \tag{25}$$

Therefore, the value of $\hat{\mu}(\chi(t_s))$ can be obtained subsequently. That is to say, with the initial value of $\hat{W}_c$ and $\chi(t)$ provided, $\hat{\mu}(\chi(t_s))$ can be updated in a corresponding manner. In addition, the process of NN-enabled optimal tracking control algorithm is demonstrated within the framework of Algorithm 1.

B. Design of Online Fault Compensation

Referring to the implementation analyzed in the last section, the system with actuator faults will be further discussed as follows. To mitigate the impact of actuator failures, an FTTC method integrating fault compensation is devised to approximate $\hat{\mu}(\chi)$.

The extended system under actuator faults is supposed to be rewritten as

$$\dot{\chi} = \boldsymbol{F}(\chi) + \boldsymbol{G}(\chi)(u - u_f). \tag{26}$$

Subsequently, an NN-based fault observer via the formulation as follows:

$$\dot{\hat{\chi}} = \boldsymbol{F}(\hat{\chi}) + \boldsymbol{G}(\hat{\chi})(u - \hat{u}_f) + \boldsymbol{A}\varepsilon \tag{27}$$

in which $\hat{u}_f$ stands for the observation of u_f and the observation gain matrix $\boldsymbol{A}$ is positive definite with appropriately matched dimensions for the system. Consider $\hat{\chi} = [\hat{\epsilon}^T, d^T]^T$ with $\hat{\epsilon} = \hat{x} - x$ as the observation state. Subsequently, let $\varepsilon = \chi - \hat{\chi}$ represent the observation error.

Based on integrating fault compensation techniques, we then develop an FTTC law u by using NN inspired by the following [34], [38]:

$$u = \hat{\mu} + \hat{u}_f \tag{28}$$

where

$$\dot{\hat{u}}_f = \Theta(\hat{\chi}^T\hat{\boldsymbol{G}}^T(\hat{\chi}) - 2\hat{\mu}^TR) \tag{29}$$

acts as the estimated actuator failure, and Θ denotes a positive learning rate. The proposed FTTC configuration with actuator faults is depicted in 1.

Remark 5: This work focuses on FTTC with actuator failures. Yet practical nonlinear systems often face more complex constraints: state constraints and actuator saturation [39], sensor faults (e.g., drift, accuracy loss) degrading control performance [40], network delay and packet loss common in networked control. Future research can extend the proposed ADP framework to cover these practical cases for a more versatile FTC scheme.

Remark 6: Unlike the approach in [41], which modifies the value function by incorporating time-delay terms and additional parameters with fault compensation and optimal control not fully decoupled, the proposed FTTC strategy comprises two distinct components: optimal tracking control and fault compensation.

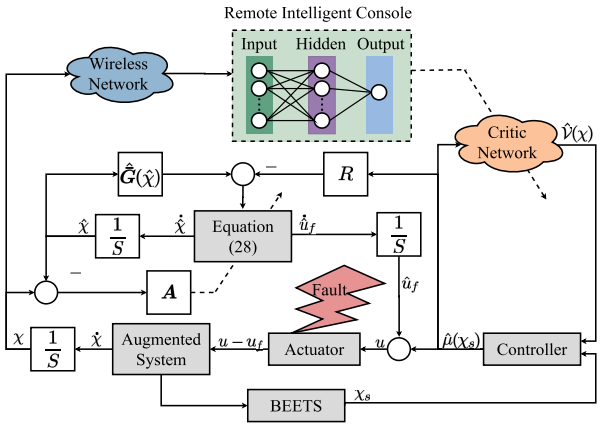

Fig. 1. FTTC configuration with actuator faults.

Notably, actuator failures are compensated in real time, eliminating the need to adjust the value function and circumventing the introduction of extra design parameters.

Before proving the UUB of the theorem under the proposed compensation strategy, we present the following assumptions.

Assumption 3 (See [14]): Given that $\mu^*(\chi)$ is Lipschitz continuous on the admissible set $ß(\Omega)$, for any two states $\mu^*(\chi)$ and $\mu^*(\chi_s)$ within the set, we are able to conclude that $\|\mu^*(\chi)-\mu^*(\chi_s)\| \le \delta_\mu \|\chi-\chi_s\| = \delta_\mu \|l_s\|$, where δ_μ is a positive constant.

Assumption 4 (See [37] and [42]): Supposing that the $\boldsymbol{G}(\chi_s)$ and $\boldsymbol{G}(\hat{\chi})$ are upper bounded by positive constants, respectively, i.e., $\boldsymbol{G}(\chi_s) \le b_{\boldsymbol{G}}$, $\boldsymbol{G}(\hat{\chi}) \le b_{\hat{\boldsymbol{G}}}$.

Theorem 1: Given the extended system with actuator faults (1), the value function (5), the NN-based observer (27) and Assumptions 2 and 4, the proposed FTTC law (28) ensures that the continuous-time ANS (1) remains UUB.

Proof: We choose a Lyapunov candidate function as $Ł_1 = \frac{1}{2}\hat{\chi}^T\hat{\chi} + \mathcal{V}(\hat{\chi}) + \frac{1}{2\Theta}\tilde{u}_f^T\tilde{u}_f$, where $\tilde{u}_f = u_f - \hat{u}$ denotes the fault estimation error. Furthermore, the derivative of $Ł_1$ can be calculated as

$$\dot{Ł}_1 = \hat{\chi}^T\dot{\hat{\chi}} + (\nabla\mathcal{V}(\hat{\chi}))^T\dot{\hat{\chi}} + \frac{1}{\Theta}(\dot{u}_f - \dot{\hat{u}}_f)^T\tilde{u}_f. \tag{30}$$

Through a straightforward transformation using (7) and (8), one can obtain

$$(\nabla\mathcal{V}(\hat{\chi}))^T\boldsymbol{G}(\hat{\chi}) = -2(\hat{\mu}(\hat{\chi}))^T R \tag{31}$$

and

$$(\nabla\mathcal{V}(\hat{\chi}))^T\dot{\hat{\chi}} = -\hat{\chi}^T\bar{Q}\hat{\chi} - \hat{\mu}^T(\hat{\chi})R\hat{\mu}(\hat{\chi}) + \Upsilon\mathcal{V}(\hat{\chi}). \tag{32}$$

Combining (31) and (32) into (30), it is further derived that

$$\begin{aligned}\dot{Ł}_1 &= \hat{\chi}^T(\boldsymbol{F}(\hat{\chi}) + \boldsymbol{G}(\hat{\chi})(\hat{\mu}(\hat{\chi}) + \hat{u}_f - u_f)) + (\nabla\mathcal{V}(\hat{\chi}))^T(\hat{\chi}) \\ &\quad\times(\hat{\mu}(\hat{\chi}) + \hat{u}_f - u_f) + \frac{1}{\Theta}(\dot{u}_f - \dot{\hat{u}}_f)^T\tilde{u}_f \\ &= \hat{\chi}^T\boldsymbol{F}(\hat{\chi}) + \hat{\chi}^T\boldsymbol{G}(\hat{\chi})\hat{\mu}(\hat{\chi}) + (\hat{\chi}^T + (\nabla\mathcal{V}(\hat{\chi}))^T) \\ &\quad\times\boldsymbol{G}(\hat{\chi})(\hat{u}_f - u_f) - \hat{\chi}^T\bar{Q}\hat{\chi} - \hat{\mu}(\hat{\chi})^T R\hat{\mu}(\hat{\chi}) + \Upsilon\mathcal{V}(\hat{\chi}) \\ &\quad + \frac{1}{\Theta}\dot{u}_f^T\tilde{u}_f - \frac{1}{\Theta}\dot{\hat{u}}_f^T\tilde{u}_f.\end{aligned} \tag{33}$$

Recalling $\boldsymbol{F}(\hat{\chi})$ has globally Lipschitz continuity according to Assumption 1 and the moothness of $\phi(d)$, it follows that its norm obeys the inequality $\|\boldsymbol{F}(\hat{\chi})\| \le b_{\hat{\boldsymbol{F}}}\|\hat{\chi}\|$ with a finite positive constant $b_{\hat{\boldsymbol{F}}}$. In addition, the term $\tilde{u}_f$ is assumed to be norm-bounded such that $\|\tilde{u}_f\| \le b_{u_f}$, where b_{u_f} is a positive constant.

By incorporating the above-mentioned analysis and applying Young's inequality $\mathfrak{p}^T\mathfrak{q} \le \frac{1}{2}\mathfrak{p}^T\mathfrak{p} + \frac{1}{2}\mathfrak{q}^T\mathfrak{q}$ into (30), we can derive that

$$\begin{aligned}\dot{Ł}_1 &= b_{\hat{\boldsymbol{F}}}\|\hat{\chi}\|^2 + \frac{1}{2}\|\hat{\chi}\|^2 + \frac{1}{2}b_{\hat{\boldsymbol{G}}}^2\|\hat{\mu}\|^2 \\ &\quad - \lambda_{\min}(\bar{Q})\|\hat{\chi}\|^2 - \lambda_{\min}(R)\|\hat{\mu}\|^2 + \Upsilon(\|W_c\|\,\|\varphi(\hat{\chi})\| \\ &\quad + \|\varepsilon_c(\hat{\chi})\|) + \frac{1}{2\Theta}\rho_2^2 + \frac{1}{2\Theta}b_{u_f}^2 \\ &\quad - \left(\hat{\chi}\boldsymbol{G}(\hat{\chi}) - 2(\hat{\mu}(\hat{\chi}))^T R + \frac{1}{\Theta}\dot{\hat{\mu}}_f^T\right)\tilde{u}_f\end{aligned} \tag{34}$$

in which $\lambda_{\min}(\cdot)$ denotes the minimum eigenvalue of the matrix, while $\lambda_{\max}(\cdot)$ represents its maximum eigenvalue. Both of them are real and positive due to symmetric positive-definite property of the matrices.

Substituting (29) into (34), we further deduce that

$$\begin{aligned}\dot{Ł}_1 &\le -(\lambda_{\min}(\bar{Q}) - b_{\hat{\boldsymbol{F}}} - \frac{1}{2})\|\hat{\chi}\|^2 - (\lambda_{\min}(R) - \frac{1}{2}b_{\hat{\boldsymbol{G}}}^2)\|\hat{\mu}\|^2 \\ &\quad + \frac{1}{2\Theta}(\rho_2^2 + b_{u_f}^2) + \Upsilon(\|W_c\|\,\|\varphi(\hat{\chi})\| + \|\varepsilon_c(\hat{\chi})\|) \\ &\le -\Pi_1\|\hat{\chi}\|^2 - \Pi_2\|\hat{\mu}\|^2 + \Pi_3\end{aligned} \tag{35}$$

where

$$\Pi_1 = \lambda_{\min}(\bar{Q}) - b_{\hat{\boldsymbol{F}}} - \frac{1}{2}$$

$$\Pi_2 = \lambda_{\min}(R) - \frac{1}{2}b_{\hat{\boldsymbol{G}}}^2$$

$$\Pi_3 = \frac{1}{2\Theta}(\rho_2^2 + b_{u_f}^2) + \Upsilon(\|W_c\|\,\|\varphi(\hat{\chi})\| + \|\varepsilon_c(\hat{\chi})\|).$$

In light of Assumption 2, predefined positive constants Θ, ρ_2, b_{u_f}, Υ mentioned earlier and the bounded nonnegative terms $\|W_c\|$, $\|\varphi(\hat{\chi})\|$, $\|\varepsilon_c(\hat{\chi})\|$ in single-layer NN (13), it is clear that $\Pi_3 > 0$. Therefore, it can be concluded that the derivative $\dot{Ł}_1$ is nonpositive (i.e., $\dot{Ł}_1 \le 0$) for all $\hat{\chi} \ne 0$ if the following condition:

$$\begin{cases}\lambda_{\min}(\bar{Q}) \ge b_{\hat{\boldsymbol{F}}} + \frac{1}{2} \\ \lambda_{\min}(R) \ge b_{\hat{\boldsymbol{G}}}\end{cases}$$

hold for any $\hat{\chi}$ residing outside the compact set

$$\Omega_{\hat{\chi}} = \left\{\hat{\chi} : \|\hat{\chi}\| \le \sqrt{\frac{\Pi_3}{\Pi_1}}\right\}.$$

This implies that the closed-loop system affected by actuator failures can achieve UUB under the proposed FTTC law. Consequently, Theorem 1 has been successfully proven.

C. Stability Analysis

The key conclusion of the stability analysis is summarized in Theorems 2 and 3.

Assumption 5 (See [14]): Assuming $\mathcal{V}^*(\chi)$ is continuously differentiable over its admissible set $\Im(\Omega)$, it follows that $\mathcal{V}^*(\chi)$ is upper bounded on $\Im(\Omega)$, i.e., $\mathcal{V}^*(\chi) \leq \varpi$.

Assumption 6 (See [43] and [44]): Assuming the following norm bounds hold: $\|\mu^*(\chi)\| \leq \rho_3$, $\|\hat{u}_f - u_f\| \leq \rho_4$, $\|\nabla\varphi(\chi_s)\| \leq b_\varphi$, $\|\nabla\varepsilon_c(\chi_s)\| \leq b_\varepsilon$, and $\|\delta\| \leq b_\delta$, where ρ_3, ρ_4, b_φ b_ε, and b_δ denote positive constants.

Theorem 2: Considering the optimal value function $\mathcal{V}(\chi)$, under the optimal control input $u^*(\chi)$ specified in (11) and Assumptions 4–6, the extended system in (3) is proven to satisfy UUB provided the following condition holds:

$$\lambda_{\min}(\bar{Q}) - \lambda_{\max}(R)\delta^2_{\mu^*}\frac{\lambda_{\max}(\Omega)}{\lambda_{\min}(\Omega)}\|\chi\|^2 \geq 0.$$

Proof: Since $\mathcal{V}^*(\chi)$ solves the HJB, we infer from its positive definiteness that $\mathcal{V}^*(\chi) > 0$ and therefore adopt $\mathcal{V}^*(\chi)$ as the Lyapunov function. The time derivative of $\mathcal{V}^*(\chi)$ takes the form as

$$\begin{aligned}\dot{\text{Ł}}_2 &= (\nabla\mathcal{V}^*(\chi))^T\dot{\chi}\\ &= (\mathcal{V}^*(\chi))^T(\boldsymbol{F}(\chi) + \boldsymbol{G}(\chi)(\mu^*(\chi_s) + \hat{u}_f - u_f))\\ &= (\mathcal{V}^*(\chi))^T(\boldsymbol{F}(\chi) + \boldsymbol{G}(\chi)(\mu^*(\chi) + \hat{u}_f - u_f))\\ &\quad + (\mathcal{V}^*(\chi))^T\boldsymbol{G}(\chi)(\mu^*(\chi_s) - \mu^*(\chi)).\end{aligned} \tag{36}$$

According to (8), we get

$$\begin{aligned}(\nabla\mathcal{V}^*(\chi))^T\boldsymbol{F}(\chi) &= -\chi^T\bar{Q}\chi - (\mu^*(\chi))^TR\mu^*(\chi) + \Upsilon\mathcal{V}^*(\chi)\\ &\quad - (\nabla\mathcal{V}^*(\chi))^T\boldsymbol{G}(\chi)\mu^*(\chi).\end{aligned} \tag{37}$$

Then, (36) can be rewritten as follows combined with (31):

$$\begin{aligned}\dot{\text{Ł}}_2 &= -\chi^T\bar{Q}\chi - (\mu^*(\chi))^TR\mu^*(\chi) + \Upsilon\mathcal{V}^*(\chi)\\ &\quad - 2(\mu^*(\chi))^TR(\hat{u}_f - u_f)\\ &\quad - 2(\mu^*(\chi))^TR(\mu^*(\chi_s) - \mu^*(\chi))\\ &= -\chi^T\bar{Q}\chi + (\mu^*(\chi))^TR\mu^*(\chi) + \Upsilon\mathcal{V}^*(\chi)\\ &\quad - 2(\mu^*(\chi))^TR(\hat{u}_f - u_f) - 2(\mu^*(\chi))^TR\mu^*(\chi_s)\\ &= -\chi^T\bar{Q}\chi + \Upsilon\mathcal{V}^*(\chi) - 2(\mu^*(\chi))^TR(\hat{u}_f - u_f)\\ &\quad + (\mu^*(\chi_s) - \mu^*(\chi))^TR(\mu^*(\chi_s) - \mu^*(\chi))\\ &\quad - (\mu^*(\chi_s))^TR\mu^*(\chi_s)\\ &\leq -\chi^T\bar{Q}\chi + \Upsilon\mathcal{V}^*(\chi) + (\mu^*(\chi))^TR\mu^*(\chi)\\ &\quad + ((\hat{u}_f - u_f))^TR(\hat{u}_f - u_f)\\ &\quad + (\mu^*(\chi_s) - \mu^*(\chi))^TR(\mu^*(\chi_s) - \mu^*(\chi))\\ &\quad - (\mu^*(\chi_s))^TR\mu^*(\chi_s)\end{aligned} \tag{38}$$

where we have used

$$-2(\mu^*(\chi))^TR(\hat{u}_f - u_f) \leq (\mu^*(\chi))^TR\mu^*(\chi) + ((\hat{u}_f - u_f))^TR(\hat{u}_f - u_f). \tag{39}$$

Then, we obtain

$$\begin{aligned}\dot{\text{Ł}}_2 &\leq -\lambda_{\min}(\bar{Q})\|\chi\|^2 + \Upsilon\varpi + \lambda_{\max}(R)(\rho_3^2 + \rho_4^2)\\ &\quad + \lambda_{\max}(R)\|\mu^*(\chi_s) - \mu^*(\chi)\|^2.\end{aligned} \tag{40}$$

Moreover, by observing that $t \in [t_s, t_{s+1})$, we recognize that the event-triggered condition described in (9) does not hold. Consequently, it can be concluded that

$$l_s\Omega l_s \leq \chi^T\Omega\chi \tag{41}$$

which can be further derived that

$$\lambda_{\min}(\Omega)\|l_s\|^2 \leq \lambda_{\max}(\Omega)\|\chi\|^2. \tag{42}$$

Using (42) and revoking Remark 3, it follows that:

$$\|\mu^*(\chi_s) - \mu^*(\chi)\|^2 \leq \delta^2_{\mu^*}\|l_s\|^2 \leq \delta^2_{\mu^*}\frac{\lambda_{\max}(\Omega)}{\lambda_{\min}(\Omega)}\|\chi\|^2. \tag{43}$$

Building on the preceding analysis in (40) through (43), we now derive the following key expression:

$$\begin{aligned}\dot{\text{Ł}}_2 &\leq -\lambda_{\min}(\bar{Q})\|\chi\|^2 + \Upsilon\varpi + \lambda_{\max}(R)(\rho_3^2 + \rho_4^2)\\ &\quad + \lambda_{\max}(R)\delta^2_{\mu^*}\frac{\lambda_{\max}(\Omega)}{\lambda_{\min}(\Omega)}\|\chi\|^2.\end{aligned} \tag{44}$$

Under the condition stated in Theorem 2 holds, the time derivative $\dot{\text{Ł}}_2$ satisfies $\dot{\text{Ł}}_2 \leq 0$ when

$$\|\chi\| \leq \sqrt{\frac{\mathbb{B}}{\mathbb{A}}} \tag{45}$$

where

$$\begin{aligned}\mathbb{A} &= \lambda_{\min}(\bar{Q}) - \lambda_{\max}(R)\delta^2_{\mu^*}\frac{\lambda_{\max}(\Omega)}{\lambda_{\min}(\Omega)}\|\chi\|^2\\ \mathbb{B} &= \Upsilon\varpi + \lambda_{\max}(R)(\rho_3^2 + \rho_4^2).\end{aligned}$$

Herein, the proof is finalized. It is evident that for the extended system $\chi(t)$, under the established condition in Theorem 2, convergence to a bounded neighborhood is ensured. This demonstrated that the optimal control law (11) proposed in the study guarantees the system (26) attain UUB as defined in the stability framework.

Theorem 3: Under the designed updating law for $\hat{W}_c$, the estimated optimal tracking control policy in (19), and in conjunction with Remark 3 and Assumptions 4–6, the extended system $\chi(t)$ and the weight approximation error $\tilde{W}_c$ are guaranteed to achieve UUB stability provided that

$$\begin{cases}\Lambda_1 = \lambda_{\min}(\bar{Q}) - 2\lambda_{\max}(R)\delta^2_{\mu^*}\frac{\lambda_{\max}(\Omega)}{\lambda_{\min}(\Omega)}\\ \Lambda_2 = \lambda_{\min}(\Xi)\frac{l_h}{2} - \lambda_{\max}(R)\lambda^{-2}_{\min}(R)b^2_{\boldsymbol{G}}b^2_\varphi\end{cases}$$

where Ξ denotes $([\delta\delta^T]/[(1+\delta^T\delta)^2])$.

Proof: In the context of the closed-loop system stability analysis, we define the Lyapunov function as follows:

$$\begin{aligned}\text{Ł}_3 &= \pounds_1 + \pounds_2 + \pounds_3\\ &= \mathcal{V}^*(\chi) + \mathcal{V}^*(\chi_s) + \frac{1}{2}\tilde{W}_c^T\tilde{W}_c.\end{aligned} \tag{46}$$

Within the design of the event-triggered design framework, two distinct cases are investigated next.

Scenario I ($t \in [t_s, t_{s+1})$): Due to the nontriggering of the event, the time derivative of $\mathcal{L}_2$ remains zero, and therefore we get

$$\begin{aligned}\dot{\mathcal{L}}_1 &= (\nabla \mathcal{V}^*(\chi))^T \dot{\chi} \\ &= (\mathcal{V}^*(\chi))^T (\boldsymbol{F}(\chi) + \boldsymbol{G}(\chi)(\hat{\mu}(\chi_s) + \hat{u}_f - u_f)) \\ &= (\mathcal{V}^*(\chi))^T (\boldsymbol{F}(\chi) + \boldsymbol{G}(\chi)(\mu^*(\chi) + \hat{u}_f - u_f)) \\ &\quad + (\mathcal{V}^*(\chi))^T \boldsymbol{G}(\chi)(\hat{\mu}(\chi_s) - \mu^*(\chi)). \end{aligned} \tag{47}$$

By referring back to (31) and (37), then it can be deduced that

$$\begin{aligned}\dot{\mathcal{L}}_1 &= \Upsilon \mathcal{V}^*(\chi) - \chi^T \bar{Q} \chi - (\mu^*(\chi))^T R \mu^*(\chi) \\ &\quad - 2(\mu^*(\chi))^T R(\hat{u}_f - u_f) \\ &\quad - 2(\mu^*(\chi))^T R(\hat{\mu}(\chi_s) - \mu^*(\chi)) \\ &= \Upsilon \mathcal{V}^*(\chi) - \chi^T \bar{Q} \chi - 2(\mu^*(\chi))^T R(\hat{u}_f - u_f) \\ &\quad + (\mu^*(\chi))^T R \mu^*(\chi) - 2(\mu^*(\chi))^T R(\hat{\mu}(\chi_s)) \\ &= \Upsilon \mathcal{V}^*(\chi) - \chi^T \bar{Q} \chi - 2(\mu^*(\chi))^T R(\hat{u}_f - u_f) \\ &\quad + (\mu^*(\chi) - \hat{\mu}(\chi_s))^T R(\mu^*(\chi) - \hat{\mu}(\chi_s)) \\ &\quad - (\mu^*(\chi_s))^T R \mu^*(\chi_s) \\ &\leq \Upsilon \mathcal{V}^*(\chi) - \chi^T \bar{Q} \chi + (\mu^*(\chi))^T R \mu^*(\chi) \\ &\quad + ((\hat{u}_f - u_f))^T R(\hat{u}_f - u_f) \\ &\quad + \lambda_{\max}(R) \left\| \mu^*(\chi) - \hat{\mu}(\chi_s) \right\|^2. \end{aligned} \tag{48}$$

Regarding the term $\|\mu^*(\chi) - \hat{\mu}(\chi_s)\|^2$, by using Remark 3 along with Young's inequality, we have

$$\begin{aligned}&\|\mu^*(\chi) - \hat{\mu}(\chi_s)\|^2 \\ &= \|\mu^*(\chi) - \mu^*(\chi_s) + \mu^*(\chi_s) - \hat{\mu}(\chi_s)\|^2 \\ &\leq 2 \left\| \mu^*(\chi) - \mu^*(\chi_s) \right\|^2 + 2 \left\| \mu^*(\chi_s) - \hat{\mu}(\chi_s) \right\|^2 \\ &\leq 2\delta_{\mu^*}^2 \frac{\lambda_{\max}(\Omega)}{\lambda_{\min}(\Omega)} \left\| \chi \right\|^2 + 2 \left\| \mu^*(\chi_s) - \hat{\mu}(\chi_s) \right\|^2. \end{aligned} \tag{49}$$

By making use of (15) and (19), in conjunction with Assumption 6, and defining approximation weight error as $\tilde{W}_c = W_c - \hat{W}_c$, we are then able to derive that

$$\begin{aligned}&\|\mu^*(\chi_s) - \hat{\mu}(\chi_s)\|^2 \\ &= \| -\frac{1}{2} R^{-1} \boldsymbol{G}^T(\chi_s)(\nabla \varphi^T(\chi_s) W_c + \nabla \varepsilon_c(\chi_s)) \\ &\quad - \left(-\frac{1}{2} R^{-1} \boldsymbol{G}^T(\chi_s) \nabla \varphi^T(\chi_s) \hat{W}_c \right) \|^2 \\ &= \| -\frac{1}{2} R^{-1} \boldsymbol{G}^T(\chi_s) \nabla \varphi^T(\chi_s) \tilde{W}_c \\ &\quad - \frac{1}{2} R^{-1} \boldsymbol{G}^T(\chi_s) \nabla \varepsilon_c(\chi_s) \|^2 \\ &\leq \frac{1}{2} \lambda_{\min}^{-2}(R) b_{\boldsymbol{G}}^2 b_\varphi^2 \|\tilde{W}_c\|^2 + \frac{1}{2} \lambda_{\min}^{-2}(R) b_{\boldsymbol{G}}^2 b_\varepsilon^2. \end{aligned} \tag{50}$$

Taking (49) and (50) into account, it yields that

$$\begin{aligned}\|\mu^*(\chi) - \hat{\mu}(\chi_s)\|^2 &\leq 2\delta_{\mu^*}^2 \frac{\lambda_{\max}(\Omega)}{\lambda_{\min}(\Omega)} \|\chi\|^2 + \lambda_{\min}^{-2}(R) b_{\boldsymbol{G}}^2 b_\varepsilon^2 \\ &\quad + \lambda_{\min}^{-2}(R) b_{\boldsymbol{G}}^2 b_\varphi^2 \|\tilde{W}_c\|^2. \end{aligned} \tag{51}$$

Therefore, (48) can be represented as

$$\begin{aligned}\dot{\mathcal{L}}_1 &\leq \Upsilon \varpi - \lambda_{\min}(\bar{Q}) \|\chi\|^2 + \lambda_{\max}(R)(\rho_3^2 + \rho_4^2 \\ &\quad + 2\delta_{\mu^*}^2 \frac{\lambda_{\max}(\Omega)}{\lambda_{\min}(\Omega)} \|\chi\|^2 + \lambda_{\min}^{-2}(R) b_{\boldsymbol{G}}^2 b_\varepsilon^2 \\ &\quad + \lambda_{\min}^{-2}(R) b_{\boldsymbol{G}}^2 b_\varphi^2 \|\tilde{W}_c\|^2). \end{aligned} \tag{52}$$

Now we shift our attention toward the time derivative of $\dot{\mathcal{L}}_3$ with respect to the temporal variable t

$$\begin{aligned}\dot{\mathcal{L}}_3 &= \tilde{W}_c^T \dot{\tilde{W}}_c \\ &= \tilde{W}_c^T \left(-l_h \frac{\delta \delta^T}{(1 + \delta^T \delta)^2} \tilde{W}_c + l_h \frac{\delta}{(1 + \delta^T \delta)^2} \varsigma_c \right) \\ &= -l_h \tilde{W}_c^T \frac{\delta \delta^T}{(1 + \delta^T \delta)^2} \tilde{W}_c + l_h \tilde{W}_c^T \frac{\delta}{(1 + \delta^T \delta)^2} \varsigma_c. \end{aligned} \tag{53}$$

Noting the straightforward inequality $(1 + \delta^T \delta)^2 \geq 1$, we therefore get

$$\begin{aligned}l_h \tilde{W}_c^T \frac{\delta}{(1 + \delta^T \delta)^2} \varsigma_c &\leq l_h \tilde{W}_c^T \frac{\delta}{(1 + \delta^T \delta)} \varsigma_c \\ &\leq \frac{l_h}{2} \tilde{W}_c^T \frac{\delta \delta^T}{(1 + \delta^T \delta)^2} W_c + \frac{l_h}{2} \varsigma_c^T \varsigma_c. \end{aligned} \tag{54}$$

Thus, based on Assumption 6, it can be handled as

$$\begin{aligned}\dot{\mathcal{L}}_3 &\leq -\frac{l_h}{2} \tilde{W}_c^T \frac{\delta \delta^T}{(1 + \delta^T \delta)^2} W_c + \frac{l_h}{2} \varsigma_c^T \varsigma_c \\ &\leq -\lambda_{\min}(\Xi) \frac{l_h}{2} \|\tilde{W}_c\|^2 + \frac{l_h}{2} b_\delta^2 \end{aligned} \tag{55}$$

where

$$\Xi = \frac{\delta \delta^T}{(1 + \delta^T \delta)^2}.$$

Merging (52) and (55) and subsequently recalling (46), it can be further deduced that

$$\dot{\mathrm{L}}_3 \leq -\Lambda_1 \|\chi\|^2 - \Lambda_2 \|\tilde{W}_c\|^2 + \Lambda_3 \tag{56}$$

where

$$\begin{aligned}\Lambda_1 &= \lambda_{\min}(\bar{Q}) - 2\lambda_{\max}(R)\delta_{\mu^*}^2 \frac{\lambda_{\max}(\Omega)}{\lambda_{\min}(\Omega)} \\ \Lambda_2 &= \lambda_{\min}(\Xi) \frac{l_h}{2} - \lambda_{\max}(R) \lambda_{\min}^{-2}(R) b_{\boldsymbol{G}}^2 b_\varphi^2 \\ \Lambda_3 &= \lambda_{\max}(R)(\rho_3^2 + \rho_4^2 + \lambda_{\min}^{-2}(R) b_{\boldsymbol{G}}^2 b_\varepsilon^2) \\ &\quad + \Upsilon \varpi + \frac{l_h}{2} b_\delta^2. \end{aligned}$$

Hence, we infer that $\dot{Ł}_3 \leq 0$ under the validity of Theorem 3 and provided that at least a single one of the subsequent inequality is satisfied

$$\begin{cases} \|\chi\| \geq \sqrt{\frac{\Lambda_3}{\Lambda_1}} \\ \left\|\tilde{W}_c\right\| \geq \sqrt{\frac{\Lambda_3}{\Lambda_2}}. \end{cases}$$

Scenario II ($t = t_{s+1}$): Considering the case where triggering events occur, we analysis the difference of the Lyapunov function Ł as

$$\begin{aligned} \triangle Ł = &\frac{1}{2}\tilde{W}_c^T(t_{s+1})\tilde{W}_c(t_{s+1}) - \frac{1}{2}\tilde{W}_c^T(t_{s+1}^-)\tilde{W}_c(t_{s+1}^-) \\ &+ \mathcal{V}^*(\chi(t_{s+1})) - \mathcal{V}^*(\chi(t_s)) \\ &+ \mathcal{V}^*(\chi(t_{s+1})) - \mathcal{V}^*(\chi(t_{s+1}^-)) \end{aligned} \tag{57}$$

in which $\mathcal{V}^*(\chi(t_{s+1}^-)) = \lim_{\varrho \to 0}\mathcal{V}^*(\chi(t_{s+1} - \varrho))$ with $\varrho \in (0, t_{s+1} - t_s)$.

From the results in *scenario I*, it is clearly evident that $\mathcal{V}^*(\chi(t_{s+1})) \leq \mathcal{V}^*(\chi(t_s))$ due to the continuous and monotonically decreasing nature of $\mathcal{V}^*(\cdot)$. Furthermore, for arbitrary $t \in [t_s, t_{s+1})$, if either $\|\chi\| \geq \sqrt{\frac{\Lambda_3}{\Lambda_1}}$ or $\|\tilde{W}_c\| \geq \sqrt{\frac{\Lambda_3}{\Lambda_2}}$ holds, it can be shown that $\dot{Ł}_3 = \dot{\mathcal{L}}_1 + \dot{\mathcal{L}}_3 < 0$, ensuring strict monotonic decrease of the Lyapunov function. Given that $t_{s+1} > t_{s+1-\varrho}$ for all $\varrho \in (0, t_{s+1} - t_s)$, this condition elicits

$$\mathcal{L}_1(t_{s+1}) + \mathcal{L}_3(t_{s+1}) \leq \mathcal{L}_1(t_{s+1} - \varrho) + \mathcal{L}_3(t_{s+1} - \varrho). \tag{58}$$

Based on the preceding inequality, we take the limit as $\varrho \to 0^+$ (i.e., approaching the left-hand limit at t_{s+1}) and apply the properties of limits, leading to

$$\begin{aligned} &\mathcal{L}_1(t_{s+1}) + \mathcal{L}_3(t_{s+1}) \leq \lim_{\varrho \to 0^+}(\mathcal{L}_1(t_{s+1} - \varrho) + \mathcal{L}_3(t_{s+1} - \varrho)) \\ &= \mathcal{L}_1(t_{s+1}^-) + \mathcal{L}_3(t_{s+1}^-). \end{aligned} \tag{59}$$

Thus, at the event-triggering instant t_{s+1}, we can conclude that $\triangle Ł < 0$.

Moreover, based on the analysis presented in the two prior scenarios, it is evident that the extended system χ and weight estimation error $\tilde{W}_c$ exhibit UUB under the condition in Theorem 3. Therefore, we are able to establish the Theorem.

IV. Illustrative Simulations

A. Example 1

Considering the continues-time ANS presented in (1), several associated functions are defined as follows:

$$f(x) = \begin{bmatrix} -0.5x_1 + x_2(1 + 0.5x_2^2) \\ -0.8(x_1 + x_2) + 0.5x_2(1 - 0.3x_2^2) \end{bmatrix}$$

$$g(x) = \begin{bmatrix} -0.9 \\ -0.4 \end{bmatrix}.$$

Algorithm 1: ADP-Based Optimal Control Method.

Input: initial parameters $\hat{\mu}(0)$, $\hat{u}_f(0)$, $\epsilon(0)$ and $\hat{W}_c(0)$
Output: ADP-based FTTC law $u = \hat{\mu} + \hat{u}_f$
for $t = T; t \leq T_{\max}; t = t + T$ **do**
  Compute the weight matrix $\hat{W}_c(t)$ according to Eq. (25);
  Evaluate the extended system states $\chi(t)$ based on Eq. (3) with $\hat{\mu}(t - T)$, $\hat{u}_f(t - T)$ and $\epsilon(t - T)$;
  if *the triggered criterion (9) satisfied for* $\chi(t)$ **then**
    Update $\hat{\mu}(t)$ based on Eq. (19) using the current $\hat{W}_c(t)$;
  else
    $\hat{\mu}(t) = \hat{\mu}(t - T)$;
  end
  Update the estimated actuator fault vector $\hat{u}_f(t)$ based on Eq. (29) with $\hat{W}_c(t)$;
end
Achieve the ADP-Based FTTC law u through Eq. (28);
Return u;

Moreover, the target tracking system model is established as presented in the following:

$$\phi(d) = \begin{bmatrix} 0.1\sin(2T) \\ 0.1\cos(2T) \end{bmatrix}.$$

In addition, the initial states of system, fault observation model, and tracking model are initialized to be $x(0) = [0.32, -0.48]^T$, $\hat{x}(0) = [0.6, -0.6]^T$, $d(0) = [0.053, -0.041]^T$, respectively.

Given the defined value function (5), the event-triggered scheme (9) adopted, and the positive-definite (27), the following parameters are specified: $\bar{Q} = \text{diag}[270, 40, 0, 0]$, $R = 0.01$, $\Omega = 1.2I_4$, $T = 0.01s$ and $\boldsymbol{A} = 1.66I_4$.

Since the unknown addictive actuator failure represented by $u_f(t)$, it is modeled as

$$u_f(t) = \begin{cases} 0, & 0 < t \leq 5 \\ 8\cos(\frac{t}{2\pi}), & 5 < t \leq 70. \end{cases} \tag{60}$$

Regarding the implemented Algorithm 1, the designed parameters of the critic network are set as $l_h = 0.01$, $l_c = 6$, $\Upsilon = 0.4$, and $\Theta = 17.52$. Besides, the activation function, as mentioned in (13), is given by

$$\varphi(\chi) = [\chi_1^2, \chi_2^2, \chi_3^2, \chi_4^2, \chi_1\chi_3, \chi_2\chi_4]^T$$

which is referring to [45]. Moreover, the approximated weight vector is structured as $\hat{W}_c = [\hat{W}_{c1}, \hat{W}_{c1}, \hat{W}_{c2}, \hat{W}_{c3}, \hat{W}_{c4}, \hat{W}_{c5}, \hat{W}_{c6}]^T$, initialized with $\hat{W}_c(0) = [0, 0.004, 0.001, 0.007, 0.009, 0]^T$. Under the above-mentioned settings, the simulation outcomes are then displayed in Figs 2–8. Fig. 2 depicts the convergence process of $\hat{W}_c$. Evidently, $\hat{W}_c$ ultimately converges to the value $\hat{W}_c = [0.211, 0.108, 0.001, 0.008, 0.008, 0.004]^T$. Fig. 3 gives state approximation $\hat{x}$. The state tracking paths of the system are shown in Fig. 4, demonstrating efficient tracking of reference trajectories d_1 and d_2 during the first 20 s under the desired tracking control policy.

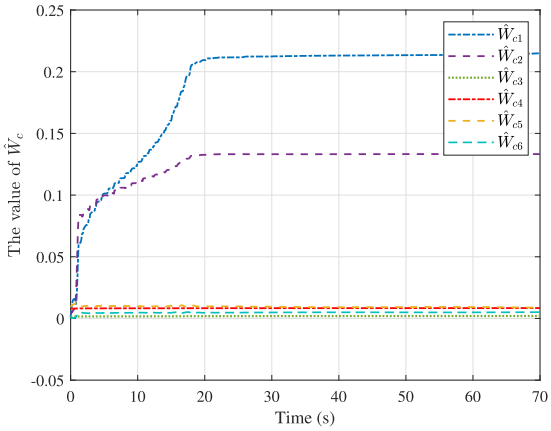

Fig. 2. Value of critic weight $\hat{W}_c$.

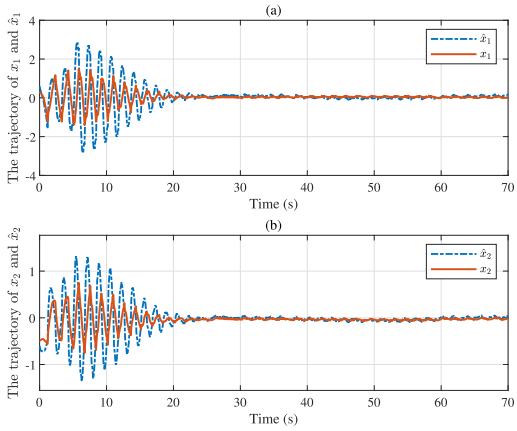

Fig. 3. State approximation of x.

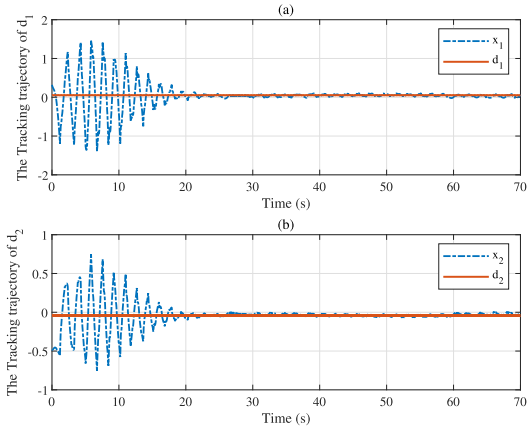

Fig. 4. State tracking trajectory of d.

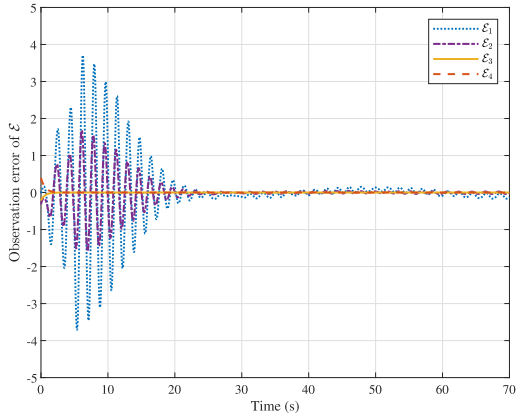

Fig. 5. Observation error $\mathcal{E}$.

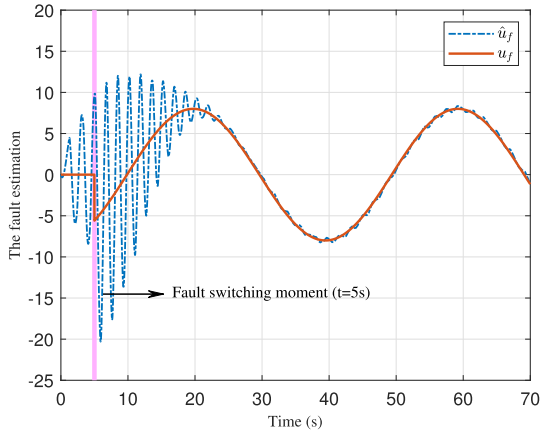

Fig. 6. Fault estimation of u_f.

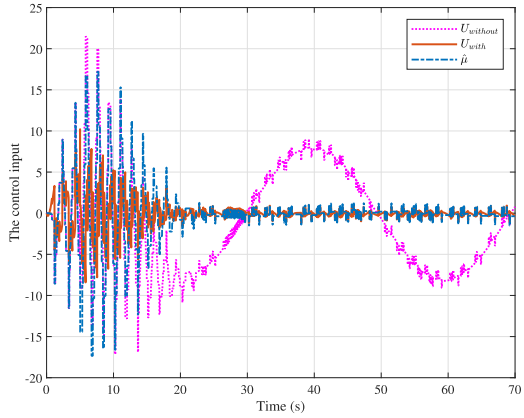

Fig. 7. Impact of fault compensation on control input trajectories.

To relieve the impact of actuator faults, a fault compensation strategy is introduced. Fig. 5 demonstrates that the observation errors eventually converge to a minuscule vicinity around zero after approximately 30 s. When actuator faults occur, the observation errors deviate momentarily but restore swiftly, indicating that the system dynamics are precisely recognized by the NN-based failure observer. Moreover, as shown in Fig. 6 at $t = 5$ s, the NN-based failure observer can approximate the faults with excellent performance.

From Fig. 7, one can notice that with fault compensation, the total approximated optimal control input U_{with} stays constant between two consecutive event-triggered intervals. However,

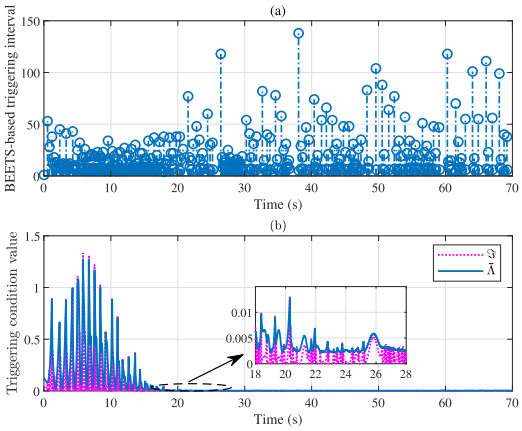

Fig. 8. (a) BEETS-driven triggering instants. (b) Two sides of the event-triggering condition.

without fault compensation, the control input U_{without} exhibits poor performance, thereby demonstrating the effectiveness of the proposed strategy. Moreover, BEETS is employed to mitigate network communication pressure. We denote the left side $\mathfrak{l}_s^T(t)\Omega l_s(t)$ as $\Im$ and the threshold $\chi^T(t_s+nT)\Omega\chi(t_s+nT)$ as $\bar{\Lambda}$. The triggering instants and two sides' value are displayed in Fig. 8, showing the data-releasing instants for BEETS. Actually, there are only 367 triggering intervals within 70 s under BEETS.

B. Example 2

To further illustrate the proposed strategy's validity, we investigate a single link robot arm system borrowed from [46]

$$\ddot{\theta}(t) = -\frac{\mathfrak{D}}{\mathfrak{g}}\dot{\theta}(t) - \frac{\mathfrak{M}g^{\circ}\mathfrak{L}}{\mathfrak{g}}\sin(\theta(t)) + \frac{u(t)-u_f(t)}{\mathfrak{g}}$$

where $\theta(t)\in\Re$ is the angle position of robot arm, $u(t)\in\Re$ is the control input, $\mathfrak{D}=2\ \text{N}\cdot\text{m}\cdot\text{s/rad}$ is the viscous friction, $\mathfrak{M}=10$ kg is the mass of payload, $\mathfrak{g}=10\ \text{kg}\cdot\text{m}^2$ is the moment of inertia, $g^{\circ}=9.81\ \text{m/s}^2$ and $\mathfrak{L}=0.5$ m is the length of the arm. The initial position satisfies that $[\theta,\dot{\theta}]=[0.52,-0.28]$. Letting $\theta=x_1$ and $\dot{\theta}=x_2$, the system thereby can be described by

$$\dot{x} = \begin{bmatrix} x_2 \\ -0.2x_2 - 4.905\sin(x_1) \end{bmatrix} + \begin{bmatrix} 0 \\ 0.1 \end{bmatrix}(u-u_f)$$

where $x=[x_1,x_2]^T$ and $x(0)=[0.52,-0.28]^T$. In this simulation, we consider another unknown actuator failure

$$u_f(t) = \begin{cases} 0, & 0<t\le 7 \\ 0.4+0.06\sin(\frac{1.2t}{5\pi}), & 7<t\le 60. \end{cases}$$

Meanwhile, the target function is chosen as

$$\phi(d) = \begin{bmatrix} 0.08\sin(3T) \\ 0.08\cos(3T) \end{bmatrix}$$

with $d(0)=[0.002,-0.001]^T$. The selected parameter values are detailed in Table I.

Fig. 9 shows the learning behavior of critic NN weights. Figs. 10 and 11 depict the observer and tracking performance,

TABLE I
PARAMETERS FOR EXAMPLE 2

Parameter	$\bar{Q}$	R	Ω	$\boldsymbol{A}$	l_h	Υ	Θ
Value	$diag[250,80,0,0]$	0.006	$1.3I_4$	$3I_4$	0.01	2.9	24.3

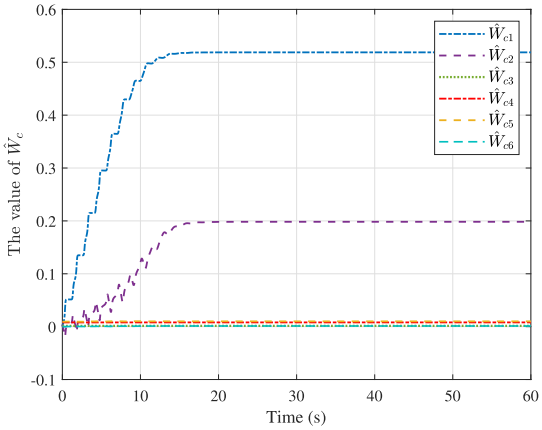

Fig. 9. Value of critic weight $\hat{W}_c$.

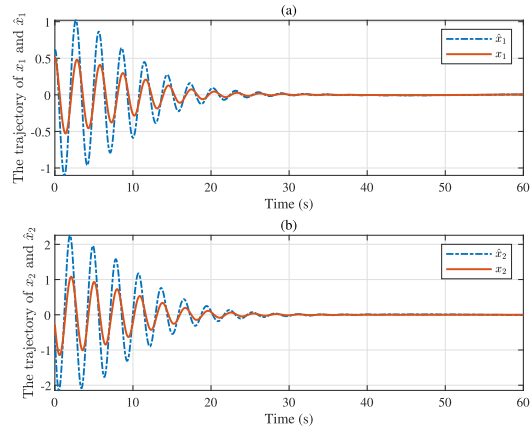

Fig. 10. State approximation of x.

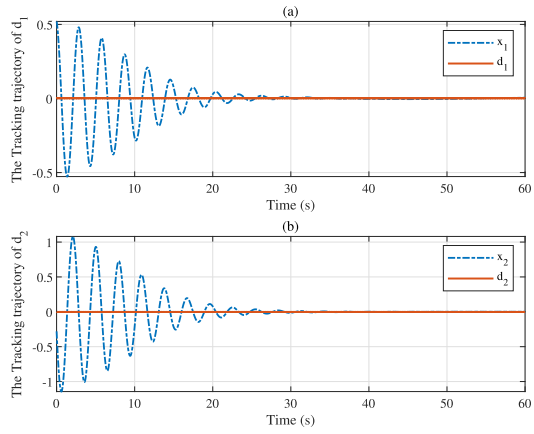

Fig. 11. State tracking trajectory of d.

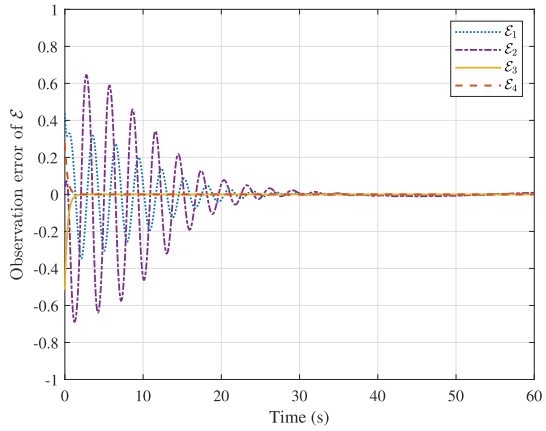

Fig. 12. Observation error $\mathcal{E}$.

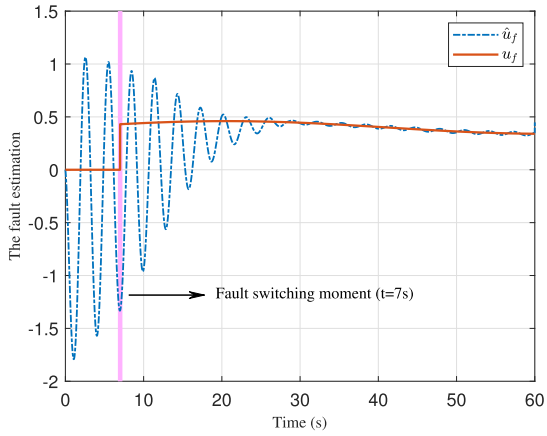

Fig. 13. Fault estimation of u_f.

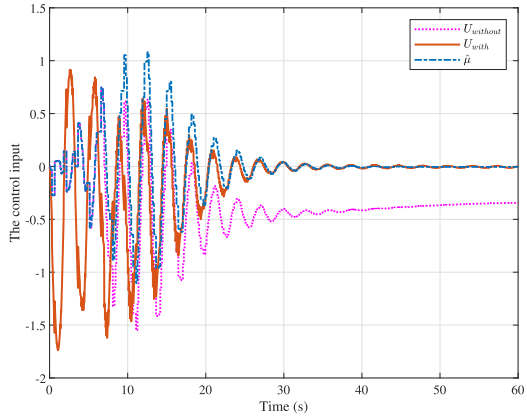

Fig. 14. Impact of fault compensation on control input trajectories.

respectively. Fig. 12 indicates observation error can converge to a neighborhood of zero in a short time while Fig. 13 illustrates fault estimation of u_f. In Fig. 14, it is readily observed that the fault compensation design holds a good performance in making control input stable. From Fig. 15, we can draw a similar conclusion as Example 1 and only 298 triggering

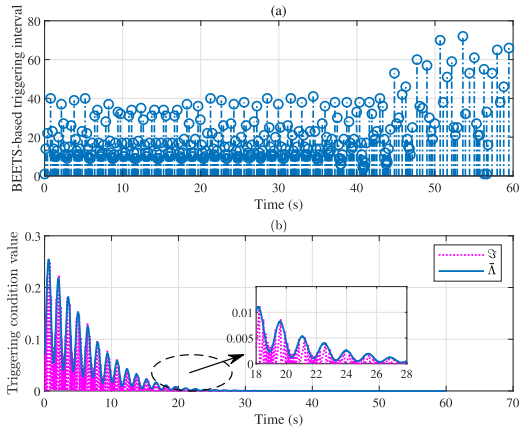

Fig. 15. (a) BEETS-driven triggering instants. (b) Two sides of the event-triggering condition.

intervals are collected in 60s. On basis of the above-mentioned analysis, the practicality of the BEETS-based control strategy is verified.

V. Conclusion

Within this article, an ADP-driven FTTC framework is proposed for ANSs experiencing actuator faults under bandwidth-constrained networks. Specifically, an extended system model integrating tracking error dynamics and desired trajectories is established for optimal control synthesis. A critic NN with adaptive weights approximates the discounted value function to solve the event-triggered HJB equation. With the aim of addressing bandwidth constraints, the proposed BEETS adaptively regulates data transmission to balance control performance and communication efficiency, while an NN-based fault observer compensates for unknown actuator faults in real time. Lyapunov analysis proves the UUB of closed-loop states, and simulations validate precise tracking, rapid fault recovery, and reduced communication load. Note that Bounemeur and Chemachema [47] addressed unknown multi-input multioutput nonlinear systems with simultaneous additive and multiplicative sensor failure, nonaffine nonlinear state-dependent actuator faults, exogenous disturbances, and unknown control directions. Future research will adopt advanced ADP to incorporate network delay and packet loss under limited bandwidth, extending the framework to such complex industrial scenarios.

References

[1] M. V. S. Sai Chandra and S. Mohapatro, "Sensor fault tolerant control in modern and green power applications: A review," *IEEE Trans. Instrum. Meas.*, vol. 73, pp. 1–24, 2024.

[2] B. Abdelhamid and C. Mohamed, "Robust fuzzy adaptive fault-tolerant control for a class of second-order nonlinear systems," *Int. J. Adaptive Control Signal Process.*, vol. 39, no. 1, pp. 15–30, 2025.

[3] T. Wang, Z. Zhao, and N. Wang, "Fault-tolerant control of stochastic strict-feedback nonlinear systems with multiple faults," *IEEE Trans. Rel.*, vol. 73, no. 3, pp. 1684–1692, Sep. 2024.

[4] Z. Yu, Y. Zhang, B. Jiang, and C. Su, *Fault-Tolerant Cooperative Control of Unmanned Aerial Vehicles*. Singapore: Springer, 2024.

[5] Y. Beyer, M. Steen, and P. Hecker, "Incremental passive fault-tolerant control for quadrotors subjected to complete rotor failures," *J. Guidance, Control, Dyn.*, vol. 46, no. 10, pp. 2033–2042, 2023.

[6] F. Rahimi, "An online fault-tolerant control approach based on policy iteration algorithm for nonlinear time-delay systems," *Int. J. Syst. Sci.*, vol. 56, no. 9, pp. 2137–2152, 2025.

[7] Y. Mi, F. Xu, X. Wang, and Y. Liu, "Maximal tolerable fault set of robust MPC for passive fault tolerance with predefined performance," *IEEE Trans. Autom. Control*, vol. 70, no. 1, pp. 611–618, Jan. 2025.

[8] Z. Jiao, X. Chen, and N. Gao, "A novel fault detection framework-based extend Kalman filter for fault-tolerant navigation system," *IEEE Trans. Rel.*, vol. 74, no. 1, pp. 2056–2068, Mar. 2025.

[9] A. Bounemeur and M. Chemachema, "Adaptive fuzzy fault-tolerant control using Nussbaum-type function with state-dependent actuator failures," *Neural Comput. Appl.*, vol. 33, no. 1, pp. 191–208, 2021.

[10] N. Li, X. Li, J. Peng, and Z. Q. Xu, "Stochastic linear quadratic optimal control problem: A reinforcement learning method," *IEEE Trans. Autom. Control*, vol. 67, no. 9, pp. 5009–5016, Sep. 2022.

[11] C. Hua, L. Li, and S. X. Ding, "Reinforcement learning-aided performance-driven fault-tolerant control of feedback control systems," *IEEE Trans. Autom. Control*, vol. 67, no. 6, pp. 3013–3020, Jun. 2022.

[12] H. Zhang, C. Zhao, and J. Ding, "Constrained reinforcement learning-based closed-loop reference model for optimal tracking control of unknown continuous-time systems," *IEEE Trans. Automat. Sci. Eng.*, vol. 21, no. 4, pp. 7312–7324, Oct. 2024.

[13] D. Li and J. Dong, "Approximate optimized backstepping control of uncertain fractional-order nonlinear systems based on reinforcement learning," *IEEE Trans. Syst., Man, Cybern. Syst.*, vol. 54, no. 11, pp. 6723–6732, Nov. 2024.

[14] J. Liu, N. Zhang, Y. Li, X. Xie, E. Tian, and J. Cao, "Learning-based event-triggered tracking control for nonlinear networked control systems with unmatched disturbance," *IEEE Trans. Syst., Man, Cybern. Syst.*, vol. 53, no. 5, pp. 3230–3240, May 2023.

[15] L. Zhang, L. Xie, Y. Jiang, Z. Li, X. Liu, and H. Su, "Optimal control for constrained discrete-time nonlinear systems based on safe reinforcement learning," *IEEE Trans. Neural Netw. Learn. Syst.*, vol. 36, no. 1, pp. 854–865, Jan. 2025.

[16] D. Wang, W. Fan, A. Liu, and J. Qiao, "Decentralized optimal neurocontroller design for mismatched interconnected systems via integral policy iteration," *IEEE Trans. Circuits Syst. II: Exp. Briefs*, vol. 71, no. 2, pp. 687–691, Feb. 2024.

[17] H. Dong, X. Zhao, and H. Yang, "Reinforcement learning-based approximate optimal control for attitude reorientation under state constraints," *IEEE Trans. Control Syst. Techol.*, vol. 29, no. 4, pp. 1664–1673, Jul. 2021.

[18] J. Yu, X. Dong, Q. Li, J. Lü, and Z. Ren, "Adaptive practical optimal time-varying formation tracking control for disturbed high-order multi-agent systems," *IEEE Trans. Circuits Syst. I: Reg. Papers*, vol. 69, no. 6, pp. 2567–2578, Jun. 2022.

[19] Q. Wei, S. Jiao, F. Wang, and Q. Dong, "Robust optimal parallel tracking control based on adaptive dynamic programming," *IEEE Trans. Cybern.*, vol. 54, no. 7, pp. 4308–4321, Jul. 2024.

[20] D. Zhang, Y. Wang, L. Meng, J. Yan, and C. Qin, "Adaptive critic design for safety-optimal FTC of unknown nonlinear systems with asymmetric constrained-input," *ISA Trans.*, vol. 155, pp. 309–318, 2024.

[21] S. Wu et al., "Co-optimization of velocity planning and energy management for intelligent plug-in hybrid electric vehicles based on adaptive dynamic programming," *IEEE Trans. Veh. Technol.*, vol. 73, no. 7, pp. 9812–9824, Jul. 2024.

[22] Q. Wei, Z. Liao, and G. Shi, "Generalized actor-critic learning optimal control in smart home energy management," *IEEE Trans. Ind. Informat.*, vol. 17, no. 10, pp. 6614–6623, Oct. 2021.

[23] Z. Yu, M. Li, Y. Zhang, and B. Jiang, "A review on safety control of unmanned," *Prog. Aerosp. Sci.*, vol. 158, 2025, Art. no. 101144.

[24] J. Liu, Y. Dong, L. Zha, X. Xie, and E. Tian, "Reinforcement learning-based tracking control for networked control systems with DoS attacks," *IEEE Trans. Inf. Forensics Secur.*, vol. 19, pp. 4188–4197, 2024.

[25] D. Meng, H. Chu, M. Tian, B. Gao, and H. Chen, "Real-time high-precision nonlinear tracking control of autonomous vehicles using fast iterative model predictive control," *IEEE Trans. Intell. Veh.*, vol. 9, no. 2, pp. 3644–3657, Feb. 2024.

[26] X. Peng, Y. He, Z. Liu, L. You, and H. Li, "Time-varying formation H_∞ tracking control and optimization for delayed multi-agent systems with exogenous disturbances," *IEEE Trans. Automat. Sci. Eng.*, vol. 22, pp. 5637–5647, 2025.

[27] H. Zeng, Z. Zhu, T. Peng, W. Wang, and X. Zhang, "Robust tracking control design for a class of nonlinear networked control systems considering bounded package dropouts and external disturbance," *IEEE Trans. Fuzzy Syst.*, vol. 32, no. 6, pp. 3608–3617, Jun. 2024.

[28] G. Su and Z. Wang, "Event-triggered robust integrated observer design for nonlinear interconnected system based on multiple intermediate estimators," *IEEE Trans. Circuits Syst. II: Exp. Briefs*, vol. 71, no. 7, pp. 3443–3447, Jul. 2024.

[29] D. Yue, E. Tian, and Q. Han, "A delay system method for designing event-triggered controllers of networked control systems," *IEEE Trans. Autom. control*, vol. 58, no. 2, pp. 475–481, Feb. 2013.

[30] Z. Gu, D. Yue, C. K. Ahn, S. Yan, and X. Xie, "Segment-weighted information-based event-triggered mechanism for networked control systems," *IEEE Trans. Cybern.*, vol. 53, no. 8, pp. 5336–5345, Aug. 2023.

[31] K. Shi et al., "Stability analysis and security-based event-triggered mechanism design for T-S fuzzy NCS with traffic congestion via DoS attack and its application," *IEEE Trans. Fuzzy Syst.*, vol. 31, no. 10, pp. 3639–3651, Oct. 2023.

[32] Z. Wu, Y. Wang, J. Xiong, and M. Xie, "Switching periodic event-triggered H_∞ control for NCSs and its application to UAVs," *IEEE Trans. Veh. Technol.*, vol. 73, no. 4, pp. 5078–5088, Apr. 2024.

[33] J. Liu, J. Ke, J. Liu, X. Xie, and E. Tian, "Reinforcement learning-boosted event-triggered reliability control for uncertain CSTR system with asymmetric constraints," *IEEE Trans. Rel.*, vol. 74, no. 1, pp. 2069–2081, Mar. 2025.

[34] H. Lin, B. Zhao, D. Liu, and C. Alippi, "Data-based fault tolerant control for affine nonlinear systems through particle swarm optimized neural networks," *IEEE/CAA J. Automatica Sinica*, vol. 7, no. 4, pp. 954–964, Jul. 2020.

[35] E. Davison and E. Kunze, "Some sufficient conditions for the global and local controllability of nonlinear time-varying systems," *SIAM J. Control*, vol. 8, no. 4, pp. 489–497, 1970.

[36] C. Qin, S. Hou, M. Pang, Z. Wang, and D. Zhang, "Reinforcement learning-based secure tracking control for nonlinear interconnected systems: An event-triggered solution approach," *Eng. Appl. Artif. Intell.*, vol. 161, 2025, Art. no. 112243.

[37] X. Liu, B. Zhao, and D. Liu, "Fault tolerant tracking control for nonlinear systems with actuator failures through particle swarm optimization-based adaptive dynamic programming," *Appl. Soft Comput.*, vol. 97, 2020, Art. no. 106766.

[38] F. Rahimi, "Dynamic event-triggered fault-tolerant control for nonlinear systems via critic learning," *J. Control Decis.*, vol. 12, no. 4, pp. 321–338, 2025.

[39] C. Qin, M. Pang, Z. Wang, S. Hou, and D. Zhang, "Observer based fault tolerant control design for saturated nonlinear systems with full state constraints via a novel event-triggered mechanism," *Eng. Appl. Artif. Intell.*, vol. 161, 2025, Art. no. 112221.

[40] A. Bounemeur, M. Chemachema, and N. Essounbouli, "Indirect adaptive fuzzy fault-tolerant tracking control for MIMO nonlinear systems with actuator and sensor failures," *ISA Trans.*, vol. 79, pp. 45–61, 2018.

[41] F. Rahimi, "Fault-tolerant control for nonlinear time-delay systems using neural network observers," *Int. J. Dyn. Control*, vol. 13, no. 1, 2025, Art. no. 33.

[42] C. Qin, X. Qiao, J. Wang, D. Zhang, Y. Hou, and S. Hu, "Barrier-critic adaptive robust control of nonzero-sum differential games for uncertain nonlinear systems with state constraints," *IEEE Trans. Syst., Man, Cybern. Syst.*, vol. 54, no. 1, pp. 50–63, Jan. 2024.

[43] J. Liu, W. Wang, B. Hu, J. Liu, X. Xie, and E. Tian, "Fuzzy-boosted event-triggered tracking control of unknown nonlinear networked systems: A PSO-driven RL approach," *IEEE Trans. Automat. Sci. Eng.*, vol. 22, pp. 7736–7747, 2025.

[44] J. Liu, N. Zhang, L. Zha, X. Xie, and E. Tian, "Reinforcement learning-based decentralized control for networked interconnected systems with communication and control constraints," *IEEE Trans. Automat. Sci. Eng.*, vol. 21, no. 3, pp. 4674–4685, Jul. 2024.

[45] J. Lin, B. Zhao, D. Liu, and Y. Wang, "Dynamic compensator-based near-optimal control for unknown nonaffine systems via integral reinforcement learning," *Neurocomputing*, vol. 564, 2024, Art. no. 126973.

[46] X. Yang, H. He, and D. Liu, "Event-triggered optimal neuro-controller design with reinforcement learning for unknown nonlinear systems," *IEEE Trans. Syst., Man, Cybern. Syst.*, vol. 49, no. 9, pp. 1866–1878, Sep. 2019.

[47] A. Bounemeur and M. Chemachema, "General fuzzy adaptive fault-tolerant control based on Nussbaum-type function with additive and multiplicative sensor and state-dependent actuator faults," *Fuzzy Sets Syst.*, vol. 468, 2023, Art. no. 108616.

Jian Liu (Member, IEEE) received the Ph.D. degree in signal and information processing from the College of Communication and Information Engineering, Nanjing University of Posts and Telecommunications, Nanjing, China, in 2018.

He is currently an Associate Professor with the School of Computer and Artificial Intelligence, Nanjing University of Finance and Economics, Nanjing, China. He has authored or coauthored more than 50 papers in refereed international journals. His research interests include cyber–physical systems, networked control systems, complex dynamical networks, intelligent optimization algorithms, and network security.

Prof. Liu was the recipient of the reward of Outstanding Reviewer for many international journals, such as *Computer Networks* and *Journal of Computational Science*. He has been a Guest Editor for the special issue *Fuzzy Modeling and Fuzzy Control Systems in Mathematics*, from August 2022 to present.

Jingjing Xia received the B.S. degree in software engineering from Huaiyin Normal University, Huaian, China, in 2024. She is currently working toward the M.S. degree in software engineering with the School of Computer and Artificial Intelligence, Nanjing University of Finance and Economics, Nanjing, China.

Her research interests include networked control systems, and learning-based optimal control methods.

Lijuan Zha received the Ph.D. degree in control science and engineering from Donghua University, Shanghai, China, in 2018.

From 2017 to 2024, she was an Associate Professor with the College of Information Engineering, Nanjing University of Finance and Economics, Nanjing, China. From 2018 to 2023, she was a Postdoctoral Research Associate with the School of Mathematics, Southeast University, Nanjing, China. She is currently a Professor with the College of Science, Nanjing Forestry University, Nanjing. Her research interests include networked control systems, neural networks, and complex dynamical systems.

Jinliang Liu (Senior Member, IEEE) received the Ph.D. degree in control theory and control engineering from the School of Information Science and Technology, Donghua University, Shanghai, China, in 2011.

From 2013 to 2016, he was a Postdoctoral Research Associate with the School of Automation, Southeast University, Nanjing, China. From 2016 to 2017, he was a Visiting Researcher/Scholar with the Department of Mechanical Engineering, University of Hong Kong, Hong Kong. From 2017 to 2018, he was a Visiting Scholar with the Department of Electrical Engineering, Yeungnam University, Gyeongsan, South Korea. From 2011 to 2023, he was an Associate Professor and a Professor with the Nanjing University of Finance and Economics, Nanjing, China. In June 2023, he joined Nanjing University of Information Science and Technology, Nanjing, China, where he is currently a Professor with the School of Computer Science. His research interests include networked control systems, complex dynamical networks, and time delay systems.

Engang Tian (Senior Member, IEEE) received the B.S. degree in mathematics from Shandong Normal University, Jinan, China, in 2002, the M.Sc. degree in operations research and cybernetics from Nanjing Normal University, Nanjing, China, in 2005, and the Ph.D. degree in control theory and control engineering from Donghua University, Shanghai, China, in 2008.

From 2011 to 2012, he was a Postdoctoral Research Fellow with the Hong Kong Polytechnic University, Hong Kong. From 2015 to 2016, he was a Visiting Scholar with the Department of Information Systems and Computing, Brunel University London, Uxbridge, U.K. From 2008 to 2018, he was an Associate Professor and then a Professor with the School of Electrical and Automation Engineering, Nanjing Normal University. In 2018, he was an Eastern Scholar with the Municipal Commission of Education, Shanghai, and joined the University of Shanghai for Science and Technology, Shanghai, where he is currently a Professor with the School of Optical-Electrical and Computer Engineering. He has authored or coauthored more than 100 papers in refereed international journals. His research interests include networked control systems, cyberattack, as well as nonlinear stochastic control and filtering.